Display Technology Letters

Fabrication and Demonstration of Electrowetting Liquid Lens Arrays

Neil R. Smith, *Member, IEEE*, Linlin Hou, *Member, IEEE*, Jinlin Zhang, and Jason Heikenfeld, *Senior Member, IEEE*

***Abstract*—Reported is the fabrication and demonstration of an array of >12 000 switchable liquid microlenses, each ~ 300 μm in diameter and switchable through plano-concave to plano-convex. Electrowetting is used to modulate the contact angle of an aqueous/oil liquid system over a range of 100°, resulting in a switchable dioptric range of $-360\ \mathrm{m}^{-1}$ to $230\ \mathrm{m}^{-1}$. Compared to previous reports of single 2–6 mm electrowetting lenses, the fabrication process reported herein reduces the individual lenslet size by ~10×. To dose liquids into large arrays of these small liquid lenslets, a scalable self-assembled dosing process was developed. The completed liquid lens array has a fill factor of 50% which can be extended to >80%.**

***Index Terms*—Electrowetting, microlens array.**

I. Introduction

As OPTICAL systems become increasingly miniaturized and complex, there is a growing need for non-mechanical optical switching and tuning. An example miniaturized optical element is a microlens array, which can be utilized in 3D displays [1], photolithography [2], biomedical imaging [3], optical communications [4], homogenization of illumination [5], and tunable optical equipment such as Shack-Hartmann sensors [6], to name a few. Recently, there has been a push to make switchable lens arrays through a wide variety of techniques including but not limited to liquid crystals, pressure-actuated membranes, and hydrogels [6]–[10]. Some challenges associated with the previously reported techniques include limited focal range, slow response time, and/or the need for bulky peripherals such as syringe pumps. Electrowetting is an attractive alternate approach for optical switching and has already been demonstrated in a single liquid lens formats [11], [12]. Reported herein is the fabrication and demonstration of arrayed [13] electrowetting microlenses. Compared to previous reports of single ~2–6 mm electrowetting lenses [11], [12], the fabrication process reported herein reduces the individual lenslet size by ~10×. The fabrication process also utilizes a scalable self-assembly processes for liquid dosing. The array consists of >12 000 lenslets with radii of 300 μm, and each filled with oil ($n = 1.41$) and a lower refractive index aqueous solution ($n = 1.33$). The lenslets can achieve flat, convex, or concave profiles, all without dependence on the polarization of light. Furthermore, because the lenslet geometry is governed by surface tension, a spherical curvature is inherently favored. Lastly, for liquid systems with 180° contact angles, the zero-voltage state of the electrowetting lenslet has the potential to even form arrays of liquid spheres.

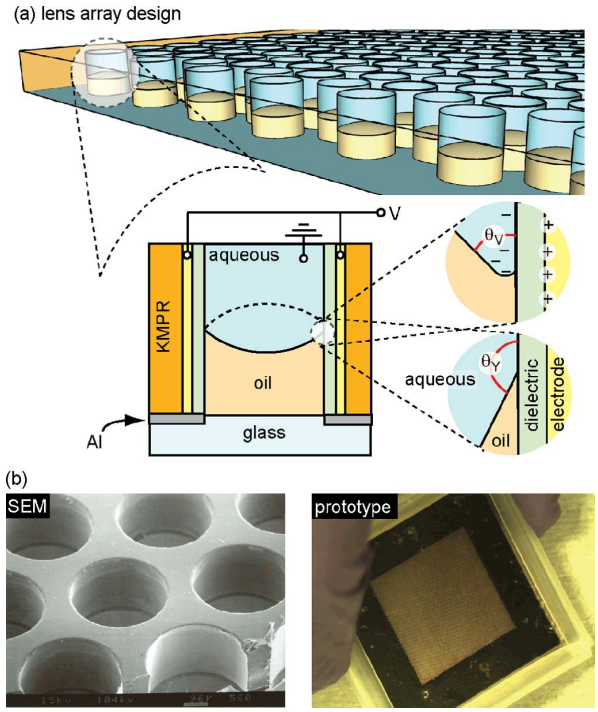


Fig. 1. (a) Diagram and operation of an electrowetting microlens array, and (b) SEM view of the lens array and photograph of the sealed lens array prototype with >12 000 lenslets.

II. Fabrication

The basic electrowetting lens array structure is shown in Fig. 1, and fabrication was performed as follows. First, a $2'' \times 2''$ wafer of Eagle 2000 glass (Corning) is metalized with a 100 nm layer of Al. Next, the aluminum is masked with positive tone photoresist (Shipley 1818) and exposed with a dose of 450 $\mathrm{mJ/cm^2}$ (365 nm). After resist development, the Al was then etched for 120 s with a phosphoric, nitric and acetic acid solution (120 parts phosphoric acid: 6 parts acetic acid: 6 parts nitric acid: 6 parts DI water by vol. %). This process revealed a hexagonal array of 300 μm radius apertures for each lenslet, and has the purpose of optically masking the non-active area

Manuscript received March 26, 2009; revised June 10, 2009. Current version published November 13, 2009. This work was supported in part by an AFOSR Young Investigator Award 06NE223 and in part by a NSF CAREER Award 0640964.

The authors are with the Novel Devices Laboratory, Department of Electrical and Computer Engineering, University of Cincinnati, Cincinnati, OH 45221 USA (e-mail: Smitn6@email.uc.edu; heikenjc@ececs.uc.edu; linlin.hou@gmail.com; zhangjilin80@gmail.com; heikenjc@email.uc.edu).

Color versions of one or more of the figures in this paper are available online at http://ieeexplore.ieee.org.

Digital Object Identifier 10.1109/JDT.2009.2027036

1551-319X/$26.00 © 2009 IEEE

between lenslets. Any remaining photoresist was then removed by solvents and oxygen plasma cleaning. Next, a 150-μm layer of Microchem KMPR 1050 negative tone resist was spin coated at a rate of 1000 rpm for 45 s. In order to eliminate the appearance of a thicker 'edge bead' of KMPR, the sample was spun in a custom-made recessed chuck. Following spinning, the sample was rested on a leveled surface in nitrogen ambient for 15 min. and then baked in a leveled oven for 10 min. at 100°C. Once the sample was cooled, the KMPR spin-coating process was repeated, and the samples were then baked for 90 min. resulting in a 300 μm thick layer of KMPR. After this second coat, the sample was cooled and immediately exposed at a dose of 2000 mJ/cm^2 (365 nm). The sample was then post-exposure baked at 100 °C for 5 min., cooled in nitrogen ambient for 15 min and then spray developed in Microchem SU-8 developer. A hard bake was then performed at 200 °C for 30 min. An SEM of the final geometrical structure of the microlens array can be seen in Fig. 1(b). This physical sidewall structure is unique compared to liquid crystal lens arrays (only liquids) or the more traditional approach of arrayed plano–convex lenslets (no sidewalls). This sidewall can be a disadvantage in the case of angled illumination. Resists like SU-8 and KMPR can typically only achieve aspect ratios of 10:1 to 20:1. Therefore, assuming a half-sphere lens shape and 300 μm radius and height, the theoretical maximum fill factor of ~91% for a hexagonal array is reduced by the sidewalls by at least another 10%. For the first demonstration reported herein the fill factor is currently ~50%.

At this point, the hexagonal array is slightly hydrophobic and could be filled with oil and water to create a permanent plano-concave lens array. However, to enable switchable lenses, electrowetting films were next deposited. First, the entire structure was sputter coated with a 150 nm layer of transparent and conducting $In_2O_3 : SnO_2$ (ITO). The ITO was then electrically insulated with ~ 1 μm layer of Parylene C prepared by chemical vapor deposition. A hydrophobic surface was then created by dip-coating in Fluoropel PFC 1601 V solution at a rate of 1 cm/sec, resting for 15 min. in a nitrogen ambient, and baking for 30 min. at 120 °C to form a 50-nm thick film. Next, liquids were dosed by self assembly. The sample was dip-coated downward through a dodecane oil film floating on aqueous solution at a rate of 0.0015 cm/s. This approach provides <5% variation in dosed volume and has been previously demonstrated for electrowetting displays [14]. However, for electrowetting lenses a novel modification to the process is needed to prevent over-filling of the lens arrays (i.e. the oil/water should each occupy only ~50% of the volume of the holes). The modification was achieved by adding a polar solvent that is soluble in both the oil and the aqueous phase, and which effectively 'swells' the oil film volume by ~2×. After self-assembly, the solvent is then extracted through diffusion by placing the sample into a large aqueous bath that is free of the solvent. The final aqueous bath also contains ~1 wt. % sodium-dodecyl-sulphate (SDS) which reduces the aqueous/oil interfacial surface tension (~5 mN/m) and therefore the required electrowetting voltage. Lastly, the lens array is sealed with a rubber gasket and a top-plate of ITO/glass in the ~1 wt. % SDS solution [Fig. 1(b)]. The above process is likely scalable to larger substrate sizes. Also, because the Parylene dielectric deposition is conformal, and because the liquid dosing is controlled by surface-tensions, the above described fabrication might be scalable to lenslets as small as only several μm in diameter. However, at such small scales the lenslet array would suffer from severe diffractive losses.

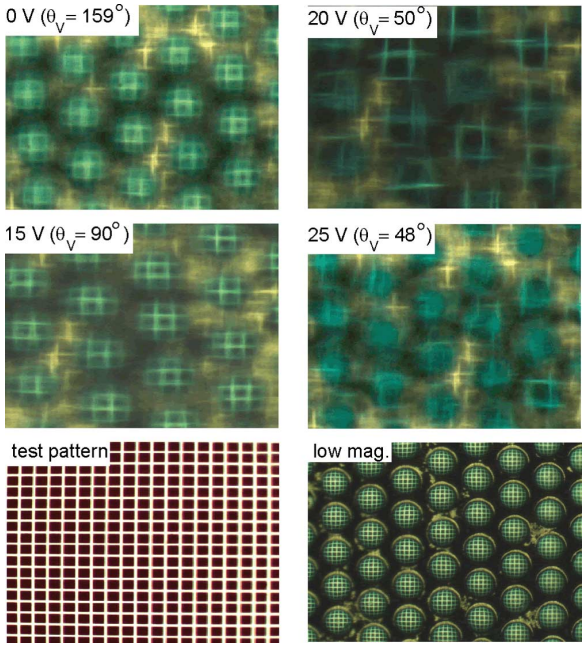


Fig. 2. Images of the lens array at 0 V (plano-concave), 15 V (almost flat response), 20 V (plano-convex), 25 V (plano-convex), the test pattern used for the lens array, and a lens array in a low magnification view (in focus).

III. Experimental Results and Discussion

An explanation of the lens array operation is now provided. An electromechanical force [15] can be applied to the aqueous liquid and thereby reduce the apparent contact angle (electrowetting). The voltage response of the contact angle (θ_V) is predicted theoretically by the electrowetting equation [16]: $\cos\theta_V = \cos\theta_Y + CV^2/2\gamma_{ao}$, where V is the applied DC or AC (RMS) voltage, θ_Y is Young's contact angle at no voltage, C is the capacitance of the Parylene/fluoropolymer (F/m^2), and γ_{ao} is the interfacial surface tension between the aqueous and oil phases. At zero-voltage, θ_Y is far greater than 90° such that the two liquids inside the lenslet to forms a plano-concave lens shape. As the voltage increases, the meniscus become flat, i.e. $\theta_V = 90°$. With the materials used herein and dodecane oil, the flat state appears at ~15 V. Next, the lenslet meniscus takes the form of a plano-convex lenslet when the voltage is increased above 15 V. The time it takes for the lenslets to switch between any two states was <2 ms (~500 Hz). This speed does not include meniscus damping, which if properly designed for the critically damped case [12] would allow a switching speed <1 ms for the case of a contact line velocity of ~10 cm/s.

Several lens array images are shown in Fig. 2, and are not representative of the actual magnification of the lens array. Instead, a focus was utilized which presented the clearest image of the lenslet operation under bias. Photographs of the lenslets were taken by imaging with a CCD, microscope, and by placing a grid of 100 μm black squares with 12.5 μm wide white lines behind the lens array (Fig. 2 test pattern). As seen in the top four images, the grid pattern appears in the Al masking between

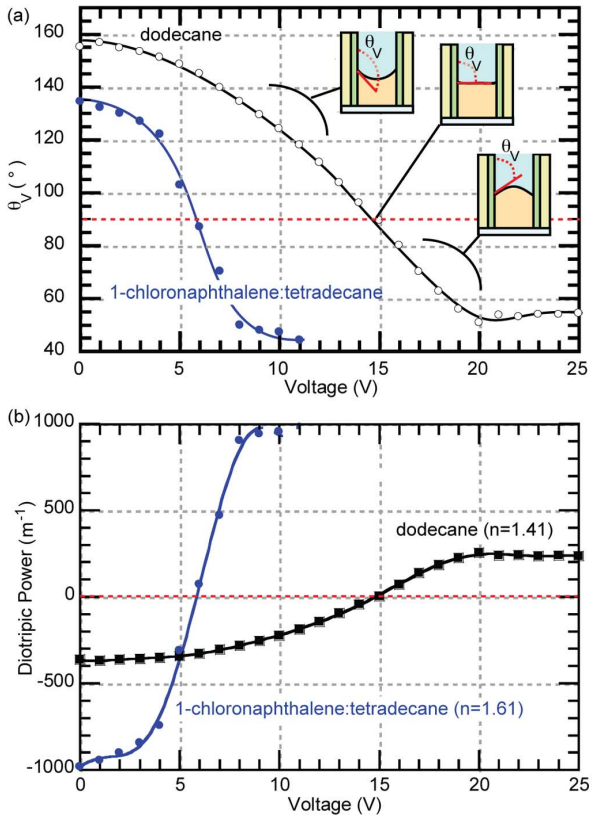


Fig. 3. (a) Measured contact angle versus voltage and (b) theoretical calculation of the dioptric power of the lens array versus voltage for use of dodecane (black data) and 1-chloronaphthalene:tetradecane (blue data) oils.

the lenslets. For some lens arrays the Al masking layer did not sufficiently block light, and can certainly be improved. At 0 V, the lens array takes on the form of a diverging lens. When the voltage is increased to 15 V, the lens array has an almost flat response (no lensing). Once the voltage increases above 15 V, the lens turns into a converging lens, magnifying the pattern. The lenslet arrays shown in Fig. 2 exhibit some optical distortion, which must be reduced for imaging applications. The dioptric power of the lens can be determined similar to that for a single electrowetting lens [12]

$$D = D_0 + \frac{(n_a - n_o)\varepsilon V^2}{n_a 2\gamma_{ao} d R_L} \tag{1}$$

where D_0 is the dioptric power of the lens when no bias is applied, n_o and n_a are the refractive index of the oil and aqueous respectively, γ_{ao} is the aqueous/oil interfacial surface tension, d is the thickness of the dielectric, ε is the dielectric constant, and R_L is the radius of the lenslet. Two different materials systems were investigated regarding the electro-optic response of the lens array: 1) dodecane/fluorpolymer/parylene as discussed previously; and 2) chloronapthalene:tetradecane [17]/fluoropolymer/$\mathrm{Al_2O_3}$. The $\mathrm{Al_2O_3}$ can be coated conformably at room temperature via atomic layer deposition, is 10X thinner than the Parylene ($\sim$100 nm), has 3X higher dielectric constant, and therefore allows for reduced operating voltage. The measured contact angle vs. voltage response in Fig. 3(a) was then combined with the optical response predicted by (1). As shown in Fig. 3(b), the achievable range for dioptric power of the individual lenses is predicted to range as much as $\pm 1000\ \mathrm{m}^{-1}$. This dioptric range compares well to the $\pm 100\ \mathrm{m}^{-1}$ dioptric ranges achieved for other switchable lens arrays [7]–[10]. The measured contact angle hysteresis was $\sim 2^{\circ}$ which will impact the repeatability of achieving various focal states of the lenslets. However, it is well known that AC bias can reduce the effective hysteresis. Although further studies are required before electrowetting lenses can be considered for practical applications, we have herein demonstrated a technique for scalable fabrication of electrowetting lens arrays, and operation over a wide range of dioptric powers at low to moderate voltages.

REFERENCES

[1] K. Choi, J. Kim, Y. Lim, and B. Lee, "Full parallax viewing-angle enhanced computer-generated holographic 3D display system using integral lens array," *Opt. Expr.*, vol. 13, pp. 10494–10502, Dec. 2005.

[2] S. Yang, C. K. Ullal, E. L. Thomas, G. Chen, and J. Aizenberg, "Microlens arrays with integrated pores as a multippattern photomask," *Appl. Phys. Lett.*, vol. 86, pp. 201121-1–201121-3, 2005.

[3] J. Kim, S. Nayak, and L. A. Lyon, "Bioresponsive hydrogel microlenses," *J. Amer. Chem. Soc.*, vol. 127, pp. 9588–9592, 2005.

[4] V. Jungnickel, A. Forck, T. Haustein, U. Kruger, V. Pohl, and C. von Helmolt, "Electronic tracking for wireless infrared communications," *IEEE Trans. Wireless Commun.*, vol. 2, no. 5, pp. 989–999, Sep. 2003.

[5] J. Pan, C. Wang, H. Lan, W. Sun, and J. Chang, "Homogenized LED-illumination using microlens arrays for pocket-sized projector," *Opt. Expr.*, vol. 15, pp. 10483–10491, 2007.

[6] Y. Hongbin, Z. Guangya, C. F. Siong, L. Feiwen, and W. Shouhua, "A tunable Shack-Hartmann wavefront sensor based on liquid-filled microlens array," *J. Micromech. Microeng.*, vol. 18, p. 105017, 2008.

[7] H. Ren, Y. Fan, and S. Wu, "Polymer network liquid crystals for tunable microlens arrays," *J. Phys. D: Appl. Phys.*, vol. 37, pp. 400–403, 2004.

[8] D. Chandra, S. Yang, and P. Lin, "Strain responsive concave and convex microlens arrays," *Appl. Phys. Lett.*, vol. 91, pp. 251912-1–251912-3, 2007.

[9] K. Jeong, G. L. Liu, N. Chronis, and L. P. Lee, "Tunable microdoublet len array," *Opt. Expr.*, vol. 12, pp. 2494–2500, 2004.

[10] B. Z. Ding and B. Ziaie, "A pH-tunable hydrogel microlens array with temperature-actuated light-switching capability," *Appl. Phys. Lett.*, vol. 94, pp. 081111-1–081111-3, 2009.

[11] B. Berge and J. Peseux, "Variable focal lens controlled by an external voltage: An application of electrowetting," *Eur. Phys. J.*, vol. 7, pp. 159–163, 2000.

[12] S. Kuiper and B. Hendriks, "Variable-focus liquid lens for miniature cameras," *Appl. Phys. Lett.*, vol. 85, pp. 1128–1130, 2004.

[13] J. Heikenfeld, N. Smith, M. Dhindsa, K. Zhou, M. Kilaru, L. Hou, J. Zhang, E. Kreit, and B. Raj, "Recent progress in arrayed electrowetting optics," *OPN*, vol. 20, pp. 20–26, 2009.

[14] B. Sun, K. Zhou, Y. Lao, J. Heikenfeld, and W. Cheng, "Scalable fabrication of electrowetting displays with self-assembled oil dosing," *Appl. Phys. Lett.*, vol. 91, pp. 011106-1–011106-3, 2007.

[15] T. B. Jones, "An electromechanical interpretation of electrowetting," *J. Micromech. Microeng.*, vol. 15, pp. 1184–1188, 2005.

[16] F. Mugele and J. C. Baret, "Electrowetting: From basics to applications," *J. Phy. Condens. Matter*, vol. 17, pp. R705–R774, 2005.

[17] J. Zhang, D. Van Meter, L. Hou, N. Smith, A. Stalcup, R. Laughlin, and J. Heikenfeld, "Preparation and analysis of 1-chloronaphthalene for highly refractive electrowetting optics," *Langmuir*, vol. 25, pp. 10413–10416, 2009.